

## Original article

## A daily time-step hydrological-energy-biomass model to estimate green roof performances across Europe to support planning and policies



Emanuele Quaranta<sup>a,\*</sup>, Ciril Arkar<sup>q</sup>, Cristina Branquinho<sup>j</sup>, Elena Cristiano<sup>d</sup>, Ricardo Cruz de Carvalho<sup>j,k</sup>, Michal Dohnal<sup>o</sup>, Ilaria Gnecco<sup>m</sup>, Dominik Gößner<sup>f</sup>, Vladimira Jelinkova<sup>n</sup>, Carmelo Maucieri<sup>c</sup>, Milena Mohri<sup>f</sup>, Panayiotis A. Nektarios<sup>g,h</sup>, Nikolaos Ntoulas<sup>i</sup>, Stefania Anna Palermo<sup>p</sup>, Anna Palla<sup>m</sup>, Patrizia Piro<sup>p</sup>, Helena Cristina Serrano<sup>j</sup>, Konstantinos X. Soulis<sup>e</sup>, Michele Turco<sup>p</sup>, Timothy Van Renterghem<sup>b</sup>, Zulema Varela<sup>j,l</sup>, Francesco Viola<sup>d</sup>, Giampaolo Zanin<sup>c</sup>, Alberto Pistocchi<sup>r</sup>

<sup>a</sup> European Commission Joint Research Centre, Ispra, Italy

<sup>b</sup> Ghent University, Department of Information Technology, WAVES Research Group, Belgium

<sup>c</sup> Department of Agronomy, Food, Natural resources, Animals and Environment (DAFNAE), University of Padova, Italy

<sup>d</sup> Dipartimento di Ingegneria Civile, Ambientale e Architettura, Università degli Studi di Cagliari, Cagliari, Italy

<sup>e</sup> Agricultural University of Athens, Department of Natural Resources Management and Agricultural Engineering, Athens, Greece

<sup>f</sup> Optigrün international AG, Krauchenwies, Germany

<sup>g</sup> Hellenic Mediterranean University, Department of Agriculture, Laboratory of Quality and Safety of Agricultural Products, Landscape and Environment, Specialization of Floriculture and Landscape Architecture, Estavromenos, Heraklion 71004, Crete, Greece

<sup>h</sup> Institute of Agri-food and Life Sciences, University Research Centre, Hellenic Mediterranean University, Heraklion 71410, Crete, Greece

<sup>i</sup> Agricultural University of Athens, Department of Crop Science, Laboratory of Floriculture and Landscape Architecture, Athens, Greece

<sup>j</sup> Center for Ecology, Evolution and Environmental Change (CE3c) & Global Change and Sustainability Institute (CHANGE), Faculdade de Ciências da Universidade de Lisboa, Portugal

<sup>k</sup> Marine and Environmental Sciences Centre (MARE), Faculdade de Ciências da Universidade de Lisboa, Portugal

<sup>l</sup> CRETUS, Ecology Unit, Department Functional Biology, Faculdade de Biología, Universidade de Santiago de Compostela, 15782 Santiago de Compostela, Spain

<sup>m</sup> Department of Civil, Chemical and Environmental Engineering, University of Genova, Genoa, Italy

<sup>n</sup> Czech Technical University in Prague, University Centre for Energy Efficient Buildings, Bustehrad, Czech Republic

<sup>o</sup> Czech Technical University in Prague, Faculty of Civil Engineering, Prague, Czech Republic

<sup>p</sup> Department of Civil Engineering, University of Calabria, 87036 Rende, CS, Italy

<sup>q</sup> University of Ljubljana, Faculty of Mechanical Engineering, Laboratory for Sustainable Technologies in Buildings, Aškerčeva 6, 1000 Ljubljana, Slovenia

<sup>r</sup> European Commission Joint Research Centre, Ispra, Italy

## ARTICLE INFO

Handling Editor: Dr Cecil Konijnendijk van den Bosch

## Keywords:

Biomass model  
Green roof  
Hydrological model  
Nature-based solutions  
Temperature model  
Urban greening

## ABSTRACT

Nature-based solutions (NBSs) and urban greening are well-established strategies used in various planning and policy instruments to promote the sustainability of cities and mitigate the effects of climate changes. Within this context, green roofs are emerging as an effective NBS in urban areas where space is often limited. The estimation of green roofs' benefits is essential for their effective implementation and engineering design. In this contribution, we present a daily time-step model to estimate the surface temperature, the growth of vegetation cover and the hydrological behaviour of a green roof. The model is tested using twenty time series of real and independent European green roofs. Results show that, in the absence of calibration, the model can reproduce the daily surface temperature with high accuracy. The vegetation growing period is also reproduced. The hydrological variables can be estimated with moderate accuracy, and higher accuracy can be achieved when the model is calibrated. Therefore, the model proves a useful tool to support the appraisal of green roofs and the planning of green infrastructures in European cities.

\* Corresponding author.

E-mail address: [Emanuele.quaranta@ec.europa.eu](mailto:Emanuele.quaranta@ec.europa.eu) (E. Quaranta).

<https://doi.org/10.1016/j.ufug.2024.128211>

Received 28 October 2022; Received in revised form 9 January 2024; Accepted 10 January 2024

Available online 15 January 2024

1618-8667/© 2024 The Author(s).

Published by Elsevier GmbH. This is an open access article under the CC BY license

(<http://creativecommons.org/licenses/by/4.0/>).

## 1. Introduction

Nature-based solutions (NBS) are increasingly applied in different planning and policy contexts, due to the numerous ecosystem services they provide (Basu, et al., 2021). Green roofs are a key NBS in the urban context. They consist of covering an impervious surface, such as the roof of a building, with a combination of layers, typically including a waterproof membrane, a drainage layer, a filter, soil substrate and vegetation (see e.g. FLL, 2018). Green roofs provide benefits at the building scale (e.g., thermal and acoustic insulation, improved microclimate, creation of recreational spaces, improved aesthetics, increased property value, prolonged lifespan of roof materials) and, when implemented at the urban scale, can deliver additional ecosystem services such as heat island mitigation, biodiversity support and urban flood control through runoff reduction (Vijayaraghavan, 2016; Quaranta et al., 2021). Therefore, green roofs are suitable to improve the resilience of cities and liveability in urban areas under a changing climate (European Commission, 2019a; Shafique et al., 2018).

In 2019, the European Commission published a strategic framework to support the deployment of green and blue roofs, drawing attention to the deployment of zero-energy buildings within the European Union (EU) from the year 2020. This EU's initiative to deploy the renovation strategy is designed to help European countries to comply with the Paris Agreement on climate change (European Commission, 2010; European Commission, 2019a; European Commission, 2019b). Urban greening is increasingly considered a strategic option (Grădinaru and Hersperger, 2019; Quaranta et al., 2022), and is referred to in the Nature Restoration Law (European Commission, 2020; Rosado-García et al., 2021).

Guidelines to design green roofs in Europe are described in Catalano et al. (2018), while the main relevant decision factors for the implementation of green roofs in Europe are discussed in Brudermann and Sangkakool (2017). European policies, incentive instruments and the share of realized green roofs in European cities are discussed in Versini et al. (2020). In Quaranta et al. (2021), the long-term (annual) benefits of urban greening are discussed in the European context, with a focus on runoff reduction, heat island mitigation and saving of energy demand for cooling during summer.

Green roof performances and benefits depend not only on climatic factors and weather characteristics, but also on vegetation type, substrate and drainage layer's properties (Quaranta et al., 2021). The behavior of green roofs has been mainly investigated by experimental and field measurements (e.g., Table 1). Simulation of green roofs entails integration of a hydrological model (to estimate the roof's substrate water content and runoff), an energy balance model (to evaluate substrate temperature) and a biomass model (to evaluate vegetation growth), and in principle requires calibration of various parameters (Djedjig et al., 2012; Quezada-Garcia et al., 2020; He and Jim, 2010; Kumar and Kaushik, 2005; Yang et al., 2015; Broekhuizen et al., 2021; Johannessen et al., 2017).

In this contribution, we examine the daily time-step model presented in Quaranta et al. (2021) (see the Method section for details). The model is conceived as a simple tool to quantify the energy and water balance and biomass growth of green roofs in the European climate. It is implemented in a MS Excel © spreadsheet that can be used in the planning and preliminary design of urban greening measures, using time series of widely available climatic variables. We compare model predictions with the observed values of twenty independent monitored green roofs in ten different climatic contexts across Europe, considering surface temperature, temperature within the green roof's soil layer, vegetation growth, soil water content and runoff (i.e., green roof outflow).

Although daily time-step models have already been used extensively (e.g., SWAT, EPIC, Quaranta et al., 2021), a daily time-step model is here validated using data from several independent green roofs in different climatic contexts across Europe, with varying characteristics of the green roof components. Furthermore, although plant growth on green

roofs has been thoroughly investigated in field experiments, to the best of our knowledge this is a first case of model verification for biomass growth in green roof systems across different contexts and with the SWAT (Soil and Water Assessment Tool) model. In the following sections, after introducing the characteristics of the model, we illustrate how the model compares with measurements in the selected case studies. The results shed lights on the strengths and limitations of the model, which are discussed in view of the intended applications of the tool.

## 2. Methods

### 2.1. Combined hydrological, biomass and energy daily time-step model

In this research, we refer to the model described in Quaranta et al. (2021). Its hydrological component has been successfully compared with measurements for agricultural soils, but not with reference to the soil layer of green roofs. A full description of the model is provided in Pistocchi et al. (2008). The hydrological balance is combined with the biomass growth model of the well-established Soil and Water Assessment Tool (SWAT) (Neitsch et al., 2011), and a surface energy balance (see Fig. 1). The model solves equations referred to a single layer of soil (unlike e.g. Quezada-Garcia et al., 2020) where the soil is described by layers).

#### 2.1.1. Hydrological model: green roof substrate water balance

The hydrological model (dashed-blue box in Fig. 1) computes the soil water balance for a specific substrate type and thickness, as in Pistocchi et al. (2008). The balance considers infiltration and saturation excess runoff, gravity drainage and actual evapotranspiration (AET). The latter is computed as a function of potential evapotranspiration (ET<sub>o</sub>) based on the Penman-Monteith equation, and available water content. The balance includes a surface water retention term,  $St$ , that we quantify for green roofs (in mm) through the equation proposed in Hansen et al. (1999) as a function of the roof slope  $i$  (-):

$$St = 2.51 - 25i + 73.3i^2 \quad (1)$$

When applying the model to green roofs, we account for irrigation as an additional equivalent precipitation. The runoff was calculated by aggregating saturation and infiltration excess and also gravity drainage.

The water balance neglects all snow processes: in Europe, these are of relevance at high latitudes and during winter, when vegetation growth is anyway mostly limited by the temperature stress factor, and this condition has not been encountered in the time series used for the validation. We did not correct precipitation to account for roof slope and wind direction, as suggested in Vanuytrecht et al. (2014). Roof slopes were mild (< 2%) in the case studies we considered, while accounting for wind effects in urban areas requires complex analysis beyond the purpose of this work.

The substrate moisture dynamics was modeled considering the well known Mualem-van Genuchten equation for hydraulic conductivity, which depends on two parameters related to the pore size distribution ( $n$ ) and the inverse of the air entry pressure ( $\alpha$ ), see Pistocchi et al. (2008) for details.

When the green roof was equipped with lateral walls, infiltration excess and the excess of surface retention did not generate runoff because of the retention effects of the lateral walls. In this case, saturation and infiltration excess was not included in the runoff calculation, but was added to the rainfall for the day after, net of the storage capacity.

#### 2.1.2. Energy balance model

The daily energy balance of the green roof surface was calculated through Eq. (2):

$$R_l + R_s - H_{AET} + H_c = \Delta G + H_r \quad (2)$$

**Table 1**  
General data of the analyzed green roofs. Temperature monitoring point measured from the substrate surface.

No.	Acronym	Latitude (°)	Altitude (m a.s.l.)	City, country	Substrate thickness (cm)	Vegetation	Average air temperature (°C), summer	Average monthly precipitation (mm)	Output	Months	Comment	Reference
1	GR8F	37.98	40	Athens, Greece	8	Tall Fescue ( <i>Festuca arundinacea</i> )	26.8	47	Hydrology, Temperature (°C) at – 4 cm	13	Irrigation with a hose for short periods was not quantified, thus assuming the same quantity as the sub-irrigation one, and this is a source of error	(Soulis et al., 2017a; 2017b)
2	GR16F	37.98	40	Athens, Greece	16	Tall Fescue ( <i>Festuca arundinacea</i> )	26.8	47	Hydrology, Temperature (°C) at – 4 cm and – 12 cm	13	See above	(Soulis et al., 2017a;2017b)
3	GR8S	37.98	40	Athens, Greece	8	<i>Sedum sediforme</i>	26.8	47	Hydrology, Temperature (°C) at – 4 cm	13	See above	(Soulis et al., 2017a; 2017b)
4	GR16S	37.98	40	Athens, Greece	16	<i>Sedum sediforme</i>	26.8	47	Hydrology, Temperature (°C) at – 4 cm and – 12 cm	13	See above	(Soulis et al., 2017b; 2017b)
5	CR5S	50.16	365	Buštěhrad, Czech Republic	5	<i>Sedum</i> mix	20.5	33	Hydrology, Temperature (°C) at – 3.5 cm	7		(Jelinkova et al., 2015; Skala et al., 2020)
6	SL4S	46.12	310	Ljubljana, Slovenia	4	<i>Sedum</i> mix	21.3	71	Temperature (°C) at the surface	11		(Arkar et al., 2018)
7	BE7S	51.14	15	Kontich, Belgium	7	<i>Sedum</i> mix	12.5 (in April)	16 (April)	Water content	1		(Van Renterghem and Botteldooren, 2014)
8	IT8F	39.3	221	Arcavacata di Rende, Italy	8	<i>Cerastium tomentosum</i> , <i>Dianthus gratianopolitanus</i> , <i>Carpobrotus edulis</i>	23.3	114	Hydrology and Surface temperature	6	Tall Fescue was used since crop data were not available.	(Palermo et al., 2019)
9	GE15G	48.0	623	Göggingen-Krauchenwies, Germany	15	Grass, lawn species	16.6	42	Temperature at – 4 cm	4	Most hydraulic parameters were not known, thus only the temperature was compared. Modelled as tall fescue.	(Gößner et al., 2021)
10	GE6S	48.0	623	Göggingen-Krauchenwies, Germany	6	<i>Sedum</i> mix	16.6	42	Temperature at – 5 cm	4	Most hydraulic parameters were not known, thus only the temperature was compared.	(Gößner et al., 2021)
11	IT8S	45.35	9	Padova, Italy	8	<i>Sedum</i> mix	24.4	72	Temp. at – 5 cm, vegetation	4	Output was only available for 6 days.	[n.a.], University of Padova
12	IT14S	45.35	9	Padua, Italy	14	<i>Sedum</i> mix	24.4	72	Temp. at – 11 cm, vegetation	4	See above	[n.a.], University of Padova
13	IT8F_b	45.35	9	Padua, Italy	8	Tall Fescue	24.4	72	Temp. at – 5 cm, vegetation	4	See above	[n.a.], University of Padova
14	IT14F	45.35	9	Padua, Italy	14	Tall Fescue	24.4	72	Temp. at – 11 cm, vegetation	4	See above	[n.a.], University of Padova
15	IT8B	45.35	9	Padua, Italy	8	Bermudagrass ( <i>Cynodon dactylon</i> )	24.4	72	Temp. at – 5 cm, vegetation	4	See above	[n.a.], University of Padova
16	IT14B	45.35	9	Padua, Italy	14	Bermudagrass ( <i>Cynodon dactylon</i> )	24.4	72 + 24	Temp. at – 11 cm, vegetation	4	See above	[n.a.], University of Padova
17	IT15A	44.4	40	Genoa, Italy	15	Alfalfa	24.3	133	Hydrology	12		(Palla et al., 2009)
18	IT30Ag	39.2	78	Cagliari, Italy	30	American Agave plants	23.4	59	Hydrology	9	LAI = 0.5, as in the ref.	(Cristiano et al., 2020)
19	PT8S	38.75	84	Lisbon, Portugal	8	<i>Sedum</i> spp	22.5	27	Water content, Temp. at - 2 cm	4	Green roof on a thick concrete layer, thermal transmittance of the support →0. Green roof age 8 years. The substrate is not as homogeneous as it was in the beginning, and in case of extreme dryness, there was no full contact of the sensor with the substrate	(Rocha, et al., 2021)
20	PT8S	38.75	84	Lisbon, Portugal	8	<i>Sedum</i> spp	21.1	15	Water content, Temp. at - 2 cm	8	Same green roof as above, but a different period	Unpublished time series (Serrano H.C., Cruz de Carvalho R., Branquinho C.)

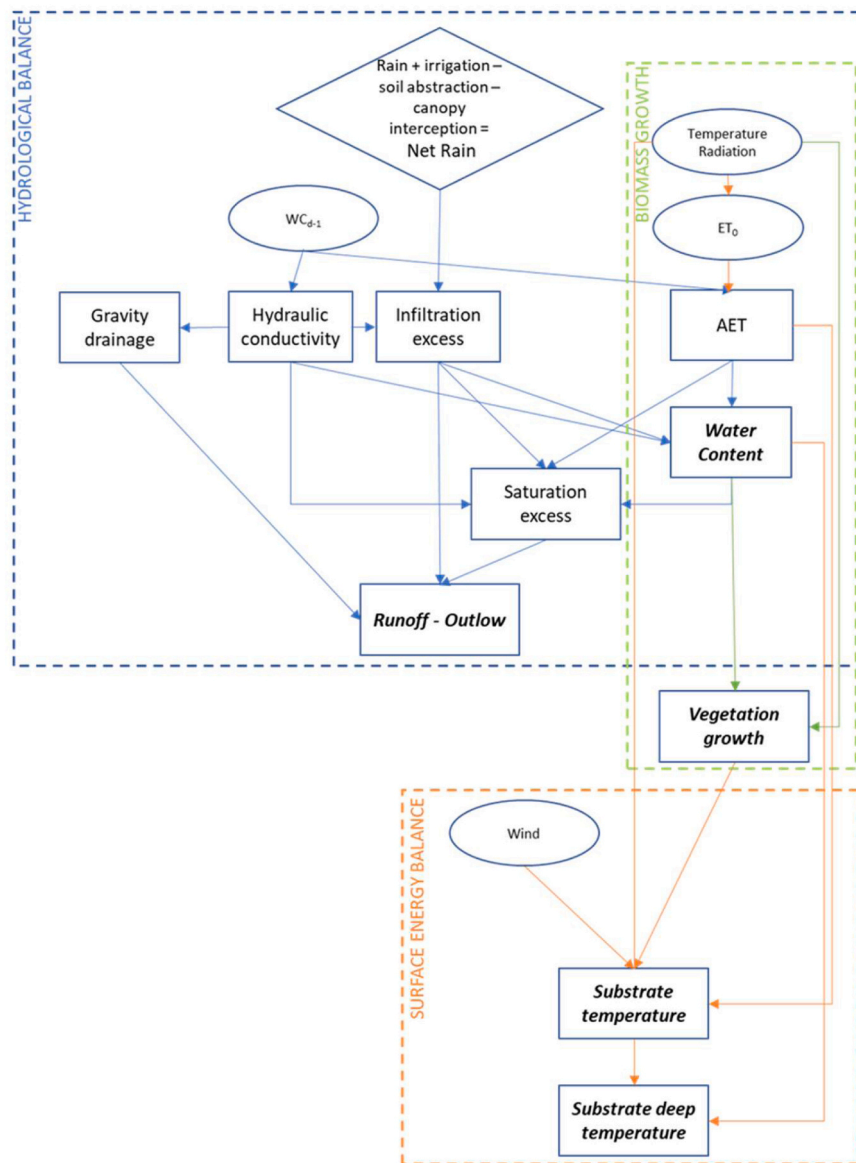


**Fig. 1.** Conceptual map of the model including the hydrologic balance, the biomass growth and energy balance flow chart. WC = water content (substrate moisture); subscript “d-1” = day before. AET= actual evapotranspiration, ET<sub>0</sub> = potential evapotranspiration. Canopy interception was set to 0 in our work.

where  $R_l$  is the net long wave radiation (i.e., considering the roof emissivity),  $R_s$  is the net short wave radiation (i.e., considering the roof's surface albedo, see below).  $H_c$  (convection heat flux) is proportional to the difference between the substrate's surface temperature (unknown,  $T_{sup}$ ) and the temperature of external air, by means of the convective air coefficient  $h_c$  ( $h_c = 10.45 \cdot W + 10W^{0.5}$ ,  $W$ =wind velocity in m/s), and  $H_r$  (flux through the roof) is proportional to the difference between the temperature of the substrate surface and the temperature below the green roof's support (e.g. the inner air temperature of a building under a green roof), by means of the thermal conductivity of the soil and support. No lateral energy flux was assumed to occur.  $\Delta G$  is the variation of the green roof's heat content (proportional to the temperature variation), assumed to be 0 as the roof is assumed to reach thermal equilibrium each day. The term  $H_{AET}$  is the latent heat of evaporation, and it is a function of AET; AET depends on  $ET_0$ , which is the evapotranspiration that would occur from an area completely and uniformly covered with growing vegetation. The output of the balance equation is the surface temperature ( $T_{sup}$ ) under steady conditions for a 1 m<sup>2</sup> surface with a substrate. Therefore,  $T_{sup}$  already takes into account the presence of vegetation, except for the shading effect. The temperature at a certain

depth of the substrate layer ( $T_{deep}$ ) was estimated after considering the thermal inertia of the substrate, depending on substrate thickness and substrate water content, as suggested in Neitsch et al. (2011). To calculate  $T_{deep}$ , we make use of a lag coefficient that controls the influence of the previous day temperature on the current day temperature (Neitsch et al., 2011). For this coefficient, ranging between 0 and 1, we selected a value of 0.5 after a few trials, as this yielded the lowest dispersion between observations and model predictions. The albedo of vegetation was set to  $\alpha_v = 0.23$  as suggested in the SWAT, while the albedo of the bare substrate was set to  $\alpha_s = 0.2$ . The overall albedo is a weighted average of  $\alpha_v$  and  $\alpha_s$  depending on the dry biomass  $bio$  (Neitsch et al., 2011). The thermal transmittance of the support of the substrate and the underneath temperature were specified input from the experiments. Eq. (2) has been already widely used in literature, e.g., Zapalovicz (2018); Quaranta et al. (2021).

### 2.1.3. Biomass growth model

The dry biomass per unit area  $bio$  (g m<sup>-2</sup>) affects the albedo of the substrate, while canopy height  $h_c$  affects the canopy and aerodynamic resistance in the  $ET_0$  term and, therefore, the actual evapotranspiration

*AET*. The daily potential dry biomass growth  $\Delta bio$  ( $\text{g m}^{-2}$ ) and canopy height were calculated using the SWAT model equations, Eq. 3 and Eq. 4 below (Neitsch et al., 2011). The biomass growth is a function of the intercepted photosynthetically active radiation (a function of daily solar radiation  $H_{\text{day}}$ ,  $\text{MJ m}^{-2}$ ), the light extinction coefficient  $k_l$ , Leaf Area Index (LAI) and radiation use efficiency  $RUE$  ( $(\text{kg ha}^{-1})(\text{MJ/m}^2)^{-1}$ ) of the plant (a function of atmospheric vapour pressure), while the canopy height on a given day is a function of the maximum canopy height  $h_c$  and the fraction of the plant's maximum LAI corresponding to a given fraction of potential heat units for the plant  $fr_{LAI_{\text{max}}}$ , as detailed in Neitsch et al. (2011).

$$\Delta bio = RUE \cdot 0.5 \cdot H_{\text{day}} (1 - e^{-k_l LAI}) \quad (3)$$

$$h_c = h_{\text{max}} \sqrt{fr_{LAI_{\text{max}}}} \quad (4)$$

The LAI development, which affects the biomass growth, was estimated as a function of fraction of growing season (cumulated heat units), as detailed in Appendix A of Neitsch et al. (2011). In our study, the cumulated heat units at maturity were set to 800 and 1000 for *Bermudagrass* and *Fescue*, as common values found in literature (see e.g. Griffith and Bamberger, 2001) and that generated good results when reproducing the biomass time series where the biomass was monitored (Appendix 1). The cumulated heat units at maturity were set to 750 and 1000 for alfalfa and *sedum*, respectively.

Depending on substrate and weather conditions, the actual dry biomass growth is calculated through appropriate temperature and water stress factors (Neitsch et al., 2011), the latter used also to correct the canopy's height growth (and the effect of the temperature is already considered in the potential heat units, which is an input of the model depending on the temperature). The substrate water balance (Section 2.1.2) provides the substrate water content used as an input to determine the water stress conditions possibly faced by the plants. Nutrient deficit and shadow effects were not considered. The model assumes that plants uniformly and totally cover the substrate; the model does not capture the wilting and the negative biomass growth. The minimum canopy height was set to 3 cm.

#### 2.1.4. Coupling of the models

The first model that is solved is the hydrological model, which depends on the meteorological conditions and soil properties, as well as on the soil's water content of the day before. The water content affects the biomass growth by means of the water stress factor, which limits biomass growth. Both the water content and the biomass load ( $\text{g m}^{-2}$ ) affect the energy model, in particular the albedo (that depends on the biomass load) and the evapotranspiration (that depends on the canopy height and water content).

### 2.2. Time series and model input data

Measurements of green roof performances were collected at sites across Europe (Fig. 2) (Table 1), ranging in latitude from  $38^\circ$  to  $51^\circ$ . The substrate thickness of the investigated green roofs ranged between 5 cm and 30 cm, and the most recurrent vegetation type was generally tall fescue (*Festuca arundinacea* Schreb.) or sedum (*Sedum* spp.). More details of the analyzed green roofs can be found in the references specified in Table 1. Table 2 summarizes the properties of the substrates. The code of each time series includes the acronym of the country, the substrate thickness in cm and the initial letter of the vegetation type.

For each site, the following meteorological variables were used at daily scale as input to the model:

- precipitation  $R$  ( $\text{mm day}^{-1}$ )
- maximum, average and minimum daily temperature  $T_{\text{max}}$ ,  $T_{\text{avg}}$  and  $T_{\text{min}}$  ( $^\circ\text{C}$ )
- wind speed  $W$  ( $\text{m s}^{-1}$ )

- daily average short wave radiation  $Rad$  ( $\text{kJ m}^{-2}$ )
- air relative humidity (%)
- net long wave radiation ( $\text{kJ m}^{-2}$ ). When not measured, it was calculated as the downward long wave radiation (by the Prata method described in Wang and Dickinson, 2013) minus the upward long wave radiation with an emissivity green roof coefficient of 0.9 (Neitsch et al., 2011)
- potential evapotranspiration,  $ET_o$  ( $\text{mm day}^{-1}$ ). When not provided, it was calculated with the Penman-Monteith equation, using the height of an herbaceous crop to compute the canopy aerodynamic resistance (Neitsch et al., 2011).
- vapour pressure  $Vap$  (hPa). When not monitored, it was calculated as suggested in Neitsch et al. (2011).

Furthermore, each green roof was characterized by its area, inclination, thickness, thermal resistance or conductivity, dry density, porosity and hydraulic properties (hydraulic conductivity at saturation, substrate water content at field capacity, FC, and at wilting point, WP, residual and saturation substrate water content, and the parameters  $\alpha$  and  $n$  of the Mualem-Van Genuchten model (see e.g., Pistocchi et al., 2008). Table 2 lists the available substrate parameters for each case study.

### 2.3. Crop type and mowing schedule

The parameters used to model the roof's vegetation ( $k_l$ ,  $RUE$ , LAI, optimal and minimum growth temperature, maximum plant height) were derived from the literature (e.g., Neitsch et al., 2011). Only time series 11–16 reported the mowing schedule, and were used for the validation. The irrigation schedule was considered.

### 2.4. Output and analysis of results

With the above selection of parameters, we computed daily runoff, average soil water content, (above ground) biomass, green roof's surface temperature ( $T_{\text{sup}}$ ) and temperature at a certain depth ( $T_{\text{deep}}$ ), which in most of the experiments was a few cm below the substrate's surface.

Table 1 shows the main characteristics of the examined green roofs and the components that could be validated, as not all the above-mentioned indicators have been measured on-site.

The soil water balance can be computed once soil hydraulic parameters are assigned. For time series No. CR5S, IT8F, IT15A, locally calibrated values for the soil hydraulic parameters were available from the original studies (Table 2). In the other cases, in principle the parameters could be calibrated on the basis of the available observations (runoff, soil water content or both). However, when the model is used for planning or preliminary design purposes, observations are not available and the parameters must be assigned a priori. Pistocchi et al. (2008) refer to five representative soil texture classes in Europe (coarse, medium, medium-fine, fine, very fine, respectively named S1, S2, S3, S4 and S5), to which they attribute average soil properties. They argue that the water balance of soils should usually be comprised within the ensemble obtained by using the hydraulic properties of the five classes. In the absence of more specific information, we compare the observed water balance (runoff and/or soil water content) with the central value of the ensemble and its range of uncertainty (i.e. its extremes) in order to evaluate the applicability of the model to unknown green roofs.

A comparison of model output and available observations for the water balance, surface temperature and biomass is drawn using the mean absolute error (MAE), the coefficient of determination  $R^2$  and the Nash–Sutcliffe model efficiency (NSME).

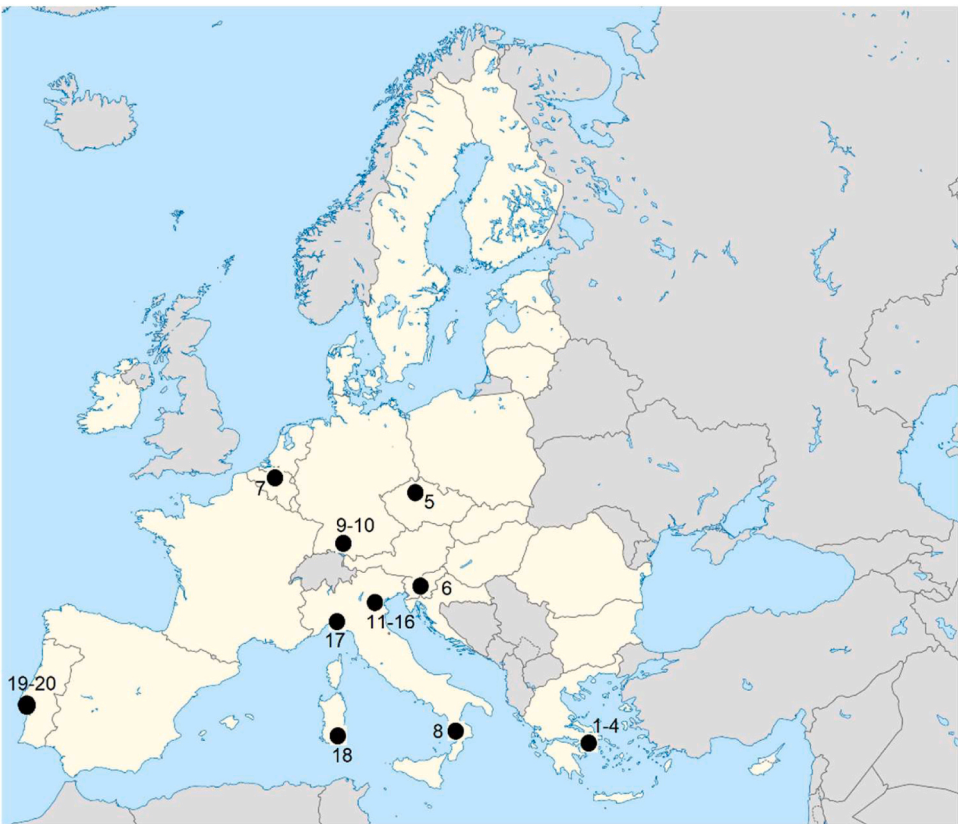


Fig. 2. Geographic distribution of the analysed green roofs. Numbers 1- 20 indicate the data series described in Table 1.

**Table 2**  
Available parameters of the substrate:  $n$  and  $\alpha$  are the Van Genuchten parameters, WP=wilting point, FC=field capacity, WC = water content (residual and at saturation), Ks conductivity at saturation. Storage capacity is thickness $\cdot$ ( WC<sub>sat</sub>- WC<sub>res</sub>).

No.	Ks (m s <sup>-1</sup> )	n	$\alpha$ (m <sup>-1</sup> )	WC <sub>res</sub>	WP	FC	WC <sub>sat</sub>	Storage capacity of substrate (cm)
1-4	1.27E-04			1%			64%	5.04 (thickness 8 cm), 10.08 (thickness 16 cm)
5	3.62E-05	1.362	3.82	5%	8%	17%	35%	1.5
6	1.27E-04			2%			88%	3.44
7	1.00E-05	1.37		3%			35%	2.24
8	3.47E-04	1.25		0%	9%	25%	58%	4.64
9							65%	
10							65%	
11-16	8.00E-04			2%	24%	36%	65%	5.04
17	5.70E-04	4.13	16.2	4%	5%	32%	46%	6.3
18	7.00E-04			2%	2.5%	25.4%	48%	13.8
19	4.10E-04				16%		33%	
20	4.10E-04				16%	33%		

3. Results

3.1. Hydrological regime

In this section, the comparison between the measured time series and the modeled ones is shown. When all the substrate’s hydraulic parameters were available (measured or calibrated by previous models), the modeled time series with these parameters was also plotted, in addition to the modelled time series using the parameters of the ensemble of the five representative European soils. Although the calibration was not the scope of our work (as it would require site-specific studies), a light calibration was performed by changing some parameters ( $n$ , conductivity, WP and FC) and checking visually the effects, until the model reproduced well the measured time series (Appendix 2). The calibrated values of parameters depend on the model and may change when a different model is implemented.

Fig. 3 shows the results for the time series whose substrate’s hydraulic parameters were available and locally calibrated in previous studies. The European soil ensemble can capture well the main trends and dynamics, enabling an appraisal of the runoff and substrate’s water content at the daily and aggregated time-scales, although the runoff is more challenging to capture (see the Discussion section for more details). The runoff predicted with the available substrate’s parameters is predicted with a MAE of 25% (time series CR5S) with respect to the measured one. Instead, the annual predicted runoff is over-estimated by a factor 1.5 (+50%) and 1.8 (+80%) in the time series IT8F and IT15A, respectively. This may be due to the fact that these parameters were calibrated on other models and may not be the optimal values for our, different, model. The NSME of the scatter plot of the daily runoff values is 0.78 for the time series No.CR5S and 0.6 for time series No.IT15A. For the time series IT8F it is – 0.74, but becomes 0.76 if only the events with runoff exceeding 5 mm are considered (representing 53% of annual

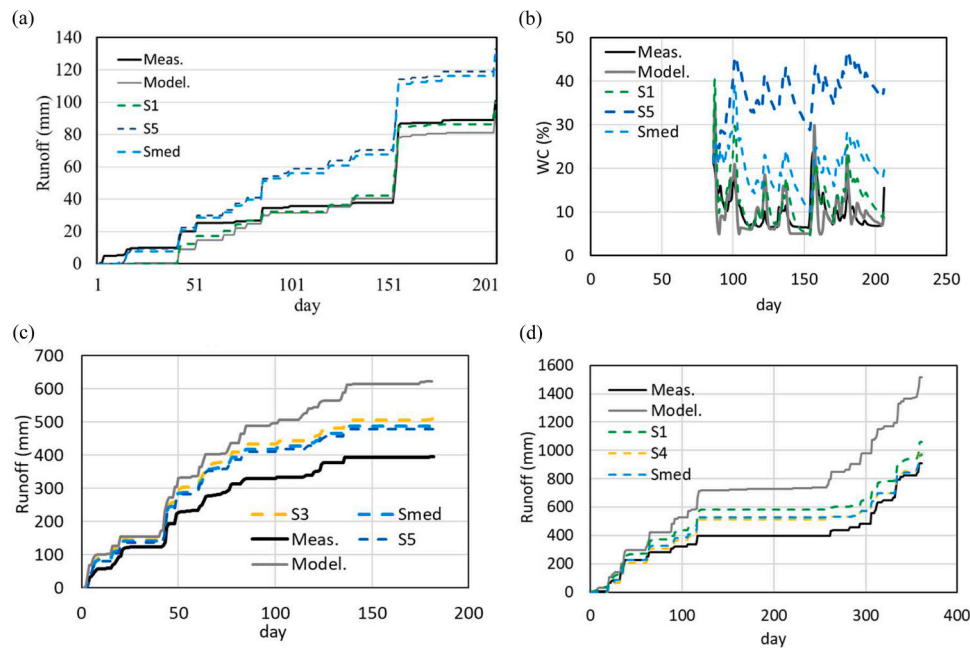


**Fig. 3.** Cumulative runoff and water content (WC) across the time series for data series CR5S (a and b), IT8F (c), IT15A (d). “Model.” means modelled data, “Meas.” means measured data, and the others refer to the representative European soils (“Smed” is the median of the results associated to the European soils).

runoff). In case of  $NSME < 0$ , but with high  $R^2$  values, results could be adequately corrected to match the measured values, by correcting them with regression equations (see, e.g., Palla et al., 2012).

Figs. 4, 5 and 6 show the results for the case studies where the locally estimated hydraulic parameters were not available and, therefore, only a comparison with the ensemble of European soils could be shown. The measured time series of water content are generally represented well by the ensemble of the European soils. Instead, the measured runoff is outside of the ensemble. Time series No. 1–4 (GR8F, GR16F, GR8S, GR16S in Table 1) came from the same site, hence the GR8S time series is representative for all of them. A well-visible discrepancy is achieved for the runoff depicted in Fig. 4: this may be due to the intensive irrigation, whose inflow contribution may be difficult to know and reproduce exactly. The irrigation was implemented with a sub-daily schedule, that cannot be simulated in our daily-step model appropriately.

The calibrated time series (Appendix 2) show that the model can capture well the main dynamics if appropriately calibrated.

### 3.2. Thermal regime

Fig. 7 represents the scatter plot of the measured temperature versus the predicted one for the GR16F site, both for the surface temperature and for the temperature within the substrate, using the calibrated values of the hydrological model (the substrate type affects these results to a very small extent, and any soil type would almost give the same results). This is a typical scatter plot for the temperatures in this study. The calculated temperatures are predicted well for all the investigated sites, with a linear coefficient of the regression equation usually around 1 (when the intercept is set to 0) and with a coefficient of determination  $R^2$  of the scatter plot above 0.8 (Table 3). The MAE is below 1%, and was calculated using units in Kelvin to be consistent with the thermal balance of the roof (e.g., long wave radiation) as in the studies reviewed in Quezada-Garcia et al. (2020).

### 3.3. Vegetation growth

The biomass model’s results were compared with monitored values for four times series (No. IT8F\_b, IT14F, IT8B, IT14B), as these were the only ones where the dry biomass per unit area and canopy height before

mowing were measured. The comparison is summarized in Figs. 8–9. There is a good agreement for cool-season turfgrass species (Fescue), and the growing process of warm-season turfgrass (Bermudagrass) is quite delayed in the model. The cumulative dry biomass is estimated with a discrepancy of 5.6%, 11.7%, 45% and 190% for time series IT8B, IT14F, IT14B and IT8F\_b, respectively. Biomass modelling is challenging on extensive green roofs systems due to the variety of plant species that can be utilized (coppices, small shrubs, succulents, turfgrasses) exhibiting different types of growth (prostrate, erect) and metabolic pathways (C3, C4, CAM<sup>1</sup>), as well as due to the negative plant response on decreasing substrate depth and irrigation regime.

## 4. Discussion

The twenty green roofs considered in our work cover a broad range of geographic contexts across Europe, as highlighted in Fig. 1, with varying latitude, distance from the sea, and altitude.

The performance of the model ensemble using the properties of the five reference European soils, in the absence of calibration, seems acceptable, considering that most of the models available in the literature are generally calibrated on the corresponding observed data (e.g., Yan et al., 2022; Liu et al., 2021). The model’s performance can be significantly improved after calibration.

### 4.1. Hydrological regime

The water content was estimated well by the hydrological model both when the substrate’s properties were known (Fig. 3) and using the ensemble of the European soils. The runoff was estimated with good accuracy as well, with NSME above 0.6 when results are compared at the daily scale. A NSME above 0.5 is generally deemed as satisfactory (Souliis et al., 2017b). The non-calibrated predicted runoff, for the time series of known parameters, was predicted with accuracy of 25% in CR5S. For

<sup>1</sup> The majority of photosynthetic plants uses C3 photosynthesis as primary mode of photosynthesis. C4 photosynthesis occurs in around 3% of vascular plants, such as crabgrass, sugarcane, corn and so on, CAM photosynthesis is the third type of photosynthesis that occurs in semi-arid plants.

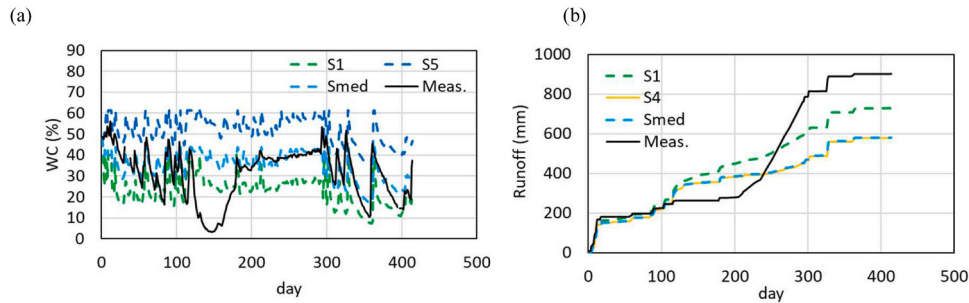


**Fig. 4.** Substrate water content (WC) (a) and cumulative runoff (b) for time series GR8S. “Meas.” means measured data, and the others refer to the average European soils (“Smed” is the median of the results associated to the European soils).

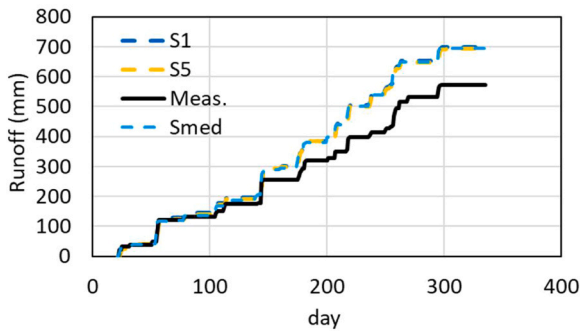


**Fig. 5.** Cumulative runoff of time series SL4S. “Meas.” means measured data, and the others refer to the average European soils (“Smed” is the median of the results associated to the European soils).

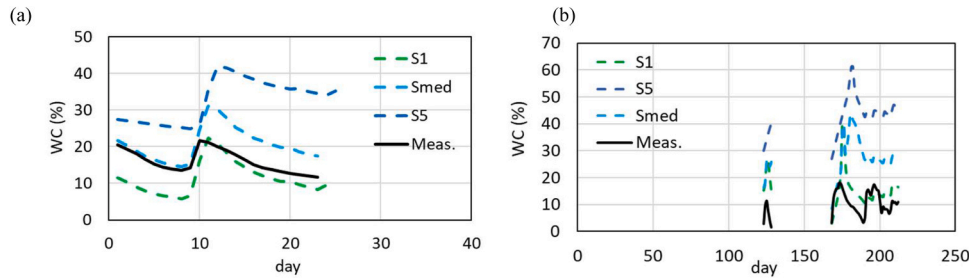


**Fig. 6.** Substrate water content (WC) for BE7S (a) and PT8S (b). “Meas.” means measured data, and the others refer to the average European soils (“Smed” is the median of the results associated to the European soils).

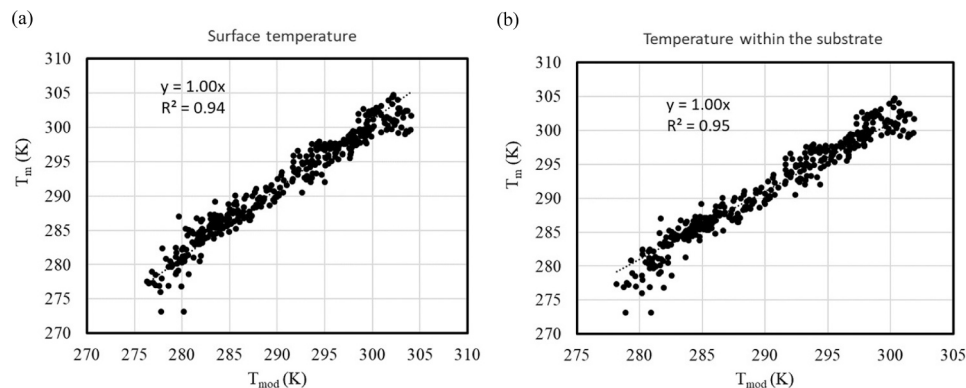


**Fig. 7.** Time series GR16F, scatter plot of the surface's temperature (a) and within the substrate's temperature (b) measured ( $T_m$ ) versus modelled ( $T_{mod}$ ).

IT8F and IT15A, the trend is captured well by the ensemble of European soils, while the annual calculated runoff is over-estimated by a factor 1.5 and 1.8, respectively, using the available substrate's parameters. This may be due to the fact that the parameter's values were calibrated in different conditions and on different models, that are not the same of our ones. Furthermore, the climate of these sites, in Italy (IT8F and IT15A), was characterized by more intense events with respect to the other time series (e.g., CR5S). The average rainfall per day (considering only rainy days) was 14.4 mm, 9.2 mm and 3.2 mm for IT8F, IT15A and CR5S, respectively.

In general, the complexity of the hydrological behavior can be expressed in three main points:

- 1) the simulation of soil hydrology is obviously sensitive to the hydraulic parameters adopted, and some of them may not reflect well the reality. Measurements of the substrate's properties made at the beginning of the experiments and hydraulic properties may have

**Table 3**

Results of the temperature validation in terms of determination coefficient ( $R^2$ ), Mean Absolute Error (MAE) and Nash–Sutcliffe model efficiency (NSME). n.a. = not available. \* = no analyses performed due to too few measurement data (six points almost with the same value), that reduces the statistical power.

Time series No.	Surface Temperature $T_{green}$			Deep Temperature $T_{deep}$		
	$R^2$	MAE (%)	NSME	$R^2$	MAE (%)	NSME
1	0.91	0.70	0.90	n.a.	n.a.	n.a.
2	0.94	0.70	0.87	0.95	0.7	0.89
3	0.91	0.60	0.91	n.a.	n.a.	n.a.
4	0.93	0.97	0.91	0.93	0.90	0.93
5	n.a.	n.a.	n.a.	0.96	0.4	0.95
6	0.96	0.80	0.91	n.a.	n.a.	n.a.
7	n.a.	n.a.	n.a.	n.a.	n.a.	n.a.
8	0.93	0.9	0.85	n.a.	n.a.	n.a.
9	n.a.	n.a.	n.a.	0.92	0.70	0.46
10	n.a.	n.a.	n.a.	0.90	0.70	0.46
11	n.a.	n.a.	n.a.	*	0.50	*
12	n.a.	n.a.	n.a.	*	0.65	*
13	n.a.	n.a.	n.a.	*	0.57	*
14	n.a.	n.a.	n.a.	*	0.64	*
15	n.a.	n.a.	n.a.	*	0.54	*
16	n.a.	n.a.	n.a.	*	0.41	*
17, 18	n.a.	n.a.	n.a.	n.a.	n.a.	n.a.
19	n.a.	n.a.	n.a.	0.87	0.58	0.85
20	n.a.	n.a.	n.a.	0.88	1.0	0.76

temporal and spatial variability. Measurements and hydraulic parameters' values were provided at a specific location and time, while the proposed model presents bulk substrate values for water content. In particular, preferential flow may occur in ways that are generally difficult to model.

- 2) The daily time step cannot characterize well the system performance in response to individual stormwater events that are typically shorter than one day, making it difficult to simulate the proper temporal variation of the substrate hydraulic conditions during stormwater events; however, for the soil water balance, usually 1 day is a fair time step, and the biggest discrepancies seem to be unrelated to storm events.
- 3) The presented model describes infiltration and saturation excess and gravity drainage, and may not be fully applicable where there is a strong effect of artificial drainage. The proposed model generally overestimates the runoff. This may be due in part to the losses associated with rainfall splashing on the vegetation and leaving the roof without having the possibility of reaching the substrate (e.g., in windy conditions). In the field experiments, leakages, losses and retention of the drainage system may reduce the runoff. In addition, the artificial drainage and impervious lining at the bottom of a green roof complicates the hydrological behaviour with respect to that of an agricultural soil.

Time series No. 1–4 (GR8F, GR16F, GR8S, GR16S, in Table 1) come from the same site. The runoff was not much affected by the substrate thickness and type of vegetation, as widely discussed in the reference scientific publications listed in Table 1, while the model, with the parameters of the European average soils, was sensitive to the substrate thickness and vegetation type. In Fig. 4, from day 130 to day 180 (April and May), water content reduces without a significant runoff; this may be due either to the significant evapotranspiration, not captured in our model, or to some inaccuracy in the data of the irrigation schedule. For time series No. 19 and 20 (PT8S), the soil water content is much lower than predicted by the model with the European soils. This seems to suggest that the model predicts a higher infiltration excess than in reality, or a much quicker drainage. Furthermore, some water content values are equal to zero: this happened because the substrate is not as homogeneous as it was in the beginning of the tests, and, in case of extreme dryness, there was no full contact of the sensor with the substrate, giving WC= 0. The green roof of the time series GR8F8 is not

further analysed, since it represents an uncommon case. The runoff was collected by two small pipes, one vertical and the other horizontal, hence the runoff was very low. A dedicated model would better simulate the outflow process and in our light calibrations it was not possible to capture the dynamics accurately.

Therefore, even when the substrate properties are fully known, the model may still require a site-specific calibration (e.g., Palla et al., 2009). Calibrations are indeed generally done in literature studies, and calibrated parameters are often different from the measured ones. For instance, the substrate hydraulic properties measured in Jelinkova et al. (2015) have been found different from the calibrated values obtained in Skala et al. (2020)<sup>2</sup> for the same green roof. Clearly, the hydrological output could be better estimated if the model would be explicitly conceived to reproduce each specific green roof with calibrated parameters. However, the calibration was out of the scope of this study, mainly focusing on providing a general tool for the assessment of green roof performances in different contexts and climates, when no field data is available for calibration.

#### 4.2. Thermal regime

When it comes to the estimation of temperature, the MAE is generally below 1% (< 3 K), better than the accuracy of the models reviewed in Quezada-Garcia et al. (2020), whose accuracy ranged between 5 K and 10 K, or 3%–6%. The coefficient  $R^2$  is generally higher than 0.80, except in a few cases where plots are a cluster of data due to the restricted range of values, but that exhibit anyway a very low MAE. Regression equations (modelled versus measured) were also determined as additional result and accuracy indicators, but not further used. In a real application, they could be used as correction factor to improve the estimation, generating scatter plots of the type  $y = x$ . Differently from our methods, the SWAT model (Neitsch et al., 2011) estimates the temperature of a bare unsealed soil as a function of solar radiation, and multiplies it by the term  $b_{cv}$  (dry biomass load) to take into account of the vegetation, with higher uncertainty. The input parameters (e.g., albedo) should be selected site-specifically for future applications, or could be improved as a function of water content (Sailor et al., 2008).

#### 4.3. Vegetation growth

Plant growth on extensive green roofs has been thoroughly investigated, such as the growth of turfgrasses (Ntoulas and Nektarios, 2015), native and endemic coppices and shrubs (Nektarios et al., 2011; Varela-Stasinopoulou et al., 2023b), alophytes (Paraskevopoulou et al., 2015) and succulents (Varela-Stasinopoulou et al., 2023a). Apart from the plant species, increasing substrate depth has been proved to directly increase plant growth, while substrate type has been indifferent in most cases. Finally, irrigation regime has a direct impact on plant biomass accumulation. However, despite the broad field research work performed on plant growth, to the best of our knowledge, this is the first case of verification of a biomass growth model on extensive green roof systems across different contexts and with the SWAT model.

Vegetation-substrate interaction is complex: biomass growth varies significantly depending on species present, plant density and root type, substrate depth, water availability, growth season length, as well as green roof management. Hence modelling biomass growth faces several challenges. The SWAT model is conceived for application at the watershed scale and large areas with intensive agricultural activity; problems in plant growth patterns may arise when applied to different systems (e.g., in small green roofs and forests) (Lai et al., 2020). Furthermore, the

<sup>2</sup> Measured values were  $WC_{res} = 0.05$  (-),  $WC_{sat} = 0.35$  (-),  $n = 1.362$  (-),  $a_{VG} = 0.0382$  (1/cm),  $K_s = 313.3$  (cm/day) versus the calibrated values  $WC_{res} = 0.05$  (-),  $WC_{sat} = 0.254$  (-),  $n = 3.08$  (-),  $a_{VG} = 0.76$  (1/cm),  $K_s = 687$  (cm/day).

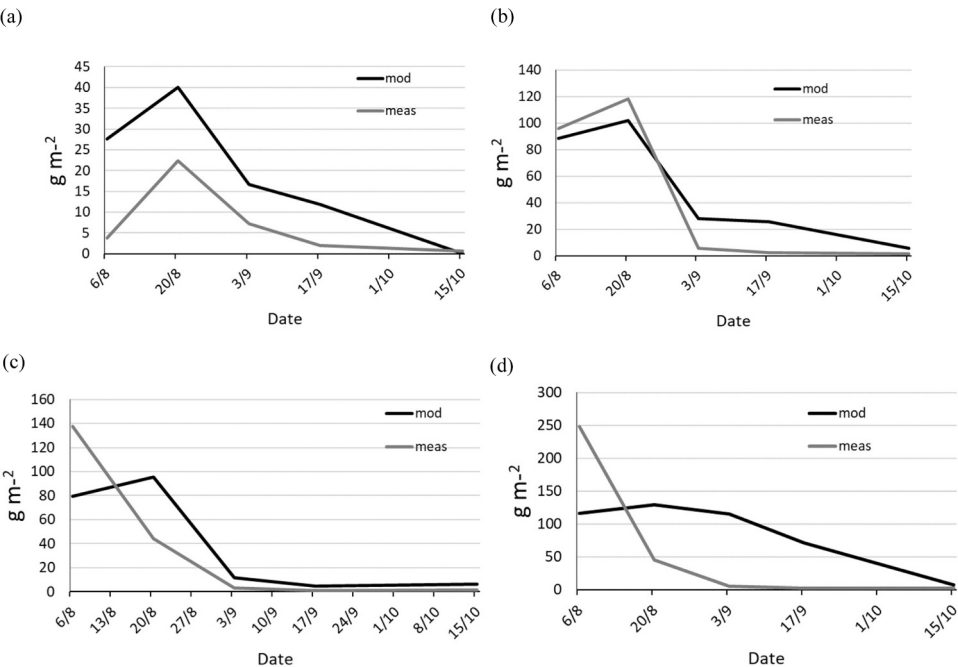


Fig. 8. Dry biomass of cut vegetation, time IT8F\_b, IT14F, IT8B, IT14B, respectively showed in the (a), (b), (c) and (d) plots.

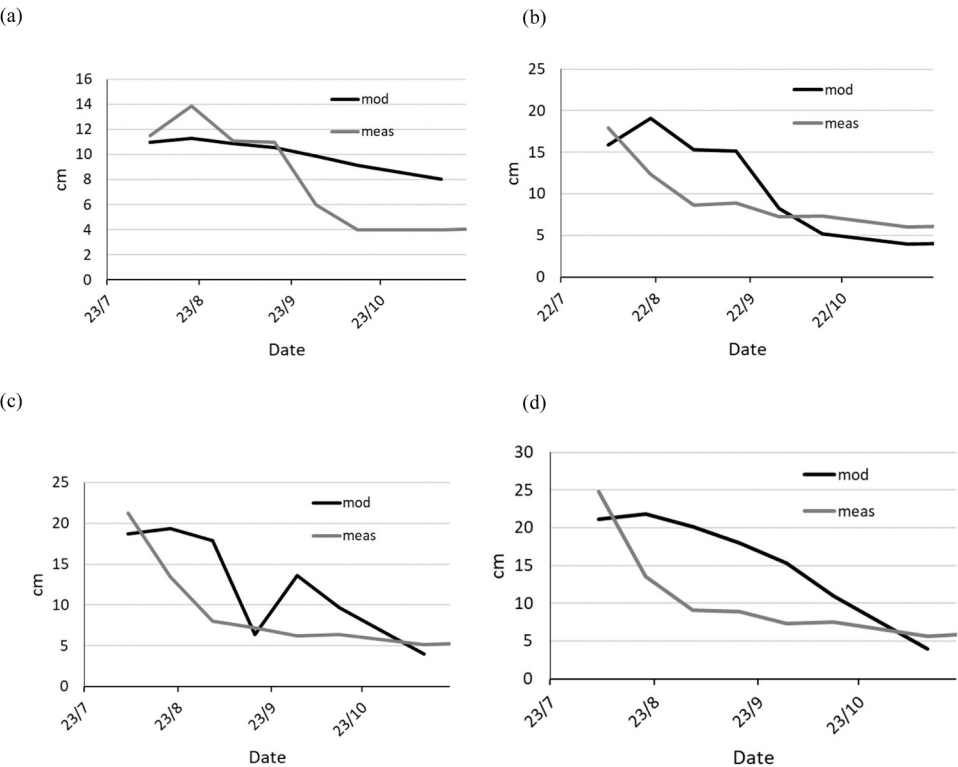


Fig. 9. Canopy's height at mowing, time series IT8F\_b, IT14F, IT8B, IT14B, respectively showed in the (a), (b), (c), and (d) plots.

vegetation cover was assumed uniform, while the predicted biomass may reflect only certain substrate portions. The model does not capture the wilting and negative biomass growth, and, after reaching the maximum theoretical height (which is an input parameter), the simulated plant biomass remains stable until the plant is harvested or killed via a management operation. Only turfgrass species have been used, rather than coppices, small shrubs or succulents.

Differences in the accuracy of the biomass growth of the two turf species by the model can be due to their strongly different physiological characteristics, that is why they were selected for the field experiments. Tall fescue is a C3, cool-season turfgrass with very good water use efficiency when grown on soils with unconfined depth, since it possesses a drought avoidance mechanism based on extending its root system in deeper soil depths and utilizing deeper water quantities. However such a mechanism cannot be utilized on the restricted shallow substrate depth profiles on an extensive green roof system. Bermudagrass has a similar drought avoidance mechanism with tall fescue, but it is a C4 warm-season turfgrass species with a higher water use efficiency (Culpepper et al., 2019). Thus, their adaptive and functional drought avoidance mechanisms can be disrupted when forced in artificial systems, like green roofs, where substrate depth is very shallow compared to soils in open field. Another difficulty lies in the intrinsic characteristics of some input data we used. For instance, heat units, also known as growing degree days, are meant to predict seasonal plant growth which not always are met because of the inaccurate or arbitrary selection of the base temperature (e.g., 5 °C, 10 °C and 15 °C were used for Bermudagrass by Patton et al. (2004), Gómez de Barreda et al. (2022) and Giolo et al. (2020), respectively), because of the different sites or the considered period and the different thermal excursion. The main vegetation parameter that affects the biomass growth is the LAI, that was estimated as a function of fraction of growing season, as detailed in Appendix A of Neitsch et al. (2011). However, the proposed generalized functions may lose accuracy when implemented site-specifically, because the modelled phenomenological grow curve, with the standard SWAT values, may not reflect very well the on-site vegetation. Therefore, biomass production should be verified during model calibration to the extent possible (Arnold, et al., 2012; Chaibou Begou, et al., 2016). Nevertheless, despite the simplifications of the SWAT model, the biomass growth was predicted well overall.

Rainfall interception by canopy was not considered. The Merriam equation could be implemented to estimate canopy interception, as described in Kozak et al. (2007). It assumes that canopy interception is a function of LAI and that maximum canopy saturation is approached exponentially as cumulative rainfall increases. If the precipitation intercepted by canopy is considered in the substrate water balance, the annual cumulative runoff would decrease by 5%, 3.8% and 3.4% for the calibrated time series CR5S, IT8F and IT15A, respectively. In Soulis et al. (2017b), the canopy interception was an additional calibration parameter. The influence of the dry biomass and canopy height on the hydrological and energy model is minimal.

Our work answers to the need of more simple simulation tools, highlighted in Quezada-García et al. (2020). The proposed mathematical model strives to be practical and simple, confirming its suitability both for large-scale appraisal of policy scenarios (e.g., Quaranta et al., 2021, 2022) and for local purposes when specifically calibrated (although an ad hoc calibration was out of the scope of the present paper), for example to optimize energy use and water management (e.g., Van Mechelen et al., 2015). When not calibrated, the model allows for a simple, but yet accurate, estimation across Europe by using the ensemble of the European representative soils.

For a general application in absence of data, the European representative soils could be used, although substrate values may differ from common soil properties (see Table 2). With reference to the green roofs tested here (Table 2), the Van Genuchten parameter  $n$  is generally  $n = 1.3$  and the residual water content is generally  $WC_{res} = 1\%$ . The Van Genuchten parameter  $\alpha$  generally ranges from 0.0083 to 0.031  $m^{-1}$  for European soils (Pistocchi et al., 2008), while the maximum one found in our cases is 16.2  $m^{-1}$ . Anyway  $\alpha$  did not affect the results appreciably and any reasonable value would be fine.

Only turfgrass species were considered, rather than coppices, small shrubs or succulents. Therefore, the growth model should be limited to turfgrasses and further research should be performed for other plant categories.

## 5. Conclusions

In this work, we implemented an integrated hydrological-energy-biomass model to estimate the performances of green roofs over a wide range of operating conditions and characteristics, covering a wide range of geographic contexts across East, South and West Europe.

In our model, the roof temperature presented a high degree of predictability, with a high correlation between estimated and monitored values ( $R^2 > 0.8$ ) and MAE below 1%. The vegetation growth could be validated only with four time series (Bermudagrass and Fescue) and proved to be in line with the monitored values. The quantification of the hydrological behavior at the daily scale is instead more complex. Nevertheless, the proposed model allows for the assessment of the hydrological behavior with reasonable accuracy when the hydrological parameters are available, and shows its potential to be calibrated for providing accurate estimations. When not calibrated, the result ensemble of the European average soils provides a reasonable estimation for general assessments and policy purposes.

The model is conceived as a flexible tool to be used in different European geographic and climatic contexts and, as such, it is expected that its accuracy is lower when compared with models conceived to simulate a specific green roof. On the other hand, very specific models fail when used outside of their context, while the current model maintains a certain degree of flexibility. The presented model can be used during the planning stage to estimate the performance of a green roof in terms of building thermal insulation and runoff reduction. Furthermore, this model can be applied during the operation stage of the building: by running the model with weekly weather forecasts, both the cooling schedule, as well as the irrigation requirement at the monthly scale, can be improved to optimize energy and water use. Finally, with the help of this model, it is possible to perform a scenario analysis in the context of urban greening for policy and strategic purposes. Future experimental research should focus on the improvement of the knowledge on thermal and botanic properties of plants to be used for modeling, and further modeling research should be performed for other plant categories in green roof systems.

## Author statement

Alberto Pistocchi developed the original version of the hydrological model and reviewed the paper. Emanuele Quaranta developed the integrated hydrological-energy-biomass model, performed the validation and wrote the paper. All the other authors provided the time series, assisted EQ during the validation and reviewed the paper. The Authors declare no conflict of interest.

## CRedit authorship contribution statement

**Van Renterghem Timothy:** Data curation, Methodology, Writing – review & editing. **Zanin Giampaolo:** Data curation, Methodology, Writing – review & editing. **Nektarios Panayiotis A.:** Data curation, Methodology, Writing – review & editing. **Quaranta Emanuele:** Conceptualization, Data curation, Formal analysis, Investigation, Methodology, Project administration, Resources, Software, Validation, Writing – original draft, Writing – review & editing. **Pistocchi Alberto:** Conceptualization, Data curation, Funding acquisition, Project administration, Resources, Software, Supervision, Writing – review & editing. **Ntoulas Nikolaos:** Data curation, Methodology, Writing – review & editing. **Arkar Ciril:** Data curation, Methodology, Writing – review & editing. **Varela Zulema:** Data curation, Methodology, Writing – review & editing. **Maucieri Carmelo:** Data curation, Methodology, Writing – review & editing. **Viola Francesco:** Data curation, Methodology, Writing – review & editing. **Mohri Milena:** Data curation, Methodology, Writing – review & editing. **Piro Patrizia:** Data curation, Methodology, Writing – review & editing. **de Carvalho Ricardo Cruz:** Data curation, Methodology, Writing – review & editing. **Serrano Helena Cristina:** Data curation, Methodology, Writing – review & editing. **Dohnal Michal:** Data curation, Methodology, Writing – review & editing. **Palermo Stefania Anna:** Data curation, Methodology, Writing – review & editing. **Branquinho Cristina:** Data curation, Methodology, Writing – review & editing. **Palla Anna:** Data curation, Methodology, Writing – review & editing. **Cristiano Elena:** Data curation, Methodology, Writing – review & editing. **Jelinkova Vladimira:** Data curation, Methodology, Writing – review & editing. **Soulis Konstantinos X.:** Data curation, Methodology, Writing – review & editing. **Gnecco Ilaria:** Data curation, Methodology, Writing – review & editing. **Turco Michele:** Data curation, Methodology, Writing – review & editing. **Gößner Dominik:** Data curation, Methodology, Writing – review & editing.

## Declaration of Competing Interest

The authors declare that they have no known competing financial interests or personal relationships that could have appeared to influence the work reported in this paper.

## Acknowledgements

Thanks to Luigi Petito of the World Green Infrastructure Network, Borut Vežočnik, Franc Rauter and Jure Sumi of Knauf Insulation, and Rudy Rossetto, who acted as contact points. Meteorological data supplied to Ricardo Cruz de Carvalho and Helena C. Serrano by Instituto Português do Mar e da Atmosfera, I. P. (IPMA). Ricardo Cruz de Carvalho was supported by a postdoctoral research grant funded by the project MedMossRoofs (PTDC/ATP-ARP/5826/2014; FCT – Foundation for Science and Technology, Portugal). The data from the lysimeter study in Athens, Greece derived from the project (Urban BioRoof) with the code number 12CHN136, funded by the Hellenic General Secretariat of Research and Innovation under the Operational Programme “Competitiveness and Entrepreneurship” (EPAN II) and by the Regional Operational Programmes of the five Regions of transitional support, under the Action “Bilateral Research and Technological Cooperation between Greece and China 2012–2014”. Z. Varela was supported by a postdoctoral research grant (I2C-B 2019) awarded by the Autonomous Government of Galicia (Xunta de Galicia, Spain). Additional support for a part of the study of V. Jelinkova was provided by the Czech Science Foundation grant no. 22-25673S. Stefania Anna Palermo is supported by the Italian Ministry of University and Research (D.M. n.1062/2021)—REACT EU—National Operational Program on Research and Innovation (PON R&I) 2014–2020—Axis IV; Action IV.4, Action IV.6. CUP: H25F21001230004. IC: 1062\_R18\_GREEN. The green roof located in the University of Calabria (Arcavacata di Rende, Italy) was co-funded by the Italian National Operative Project PON01\_02543, R&C for the convergence regions 2007/2013, I Axis; operative objective 4.1.1.1.; Action II.

## Appendix 1

The dry biomass and canopy height, measured at mowing in time series No. 13–16 (IT8F\_b, IT14F, IT8B, IT14), were used to estimate the accuracy of the biomass model.

**Table A1**

Dry biomass cut at a specific date ( $\text{g m}^{-2}$ ). Vegetation was cut at 4 cm height, and dry biomass refers to the cut one. Dry biomass was not measured for Sedum.

No.	Substrate thickness	Species	Modelled species as:	24/7	6/8	20/8	3/9	17/9	15/10
IT8B	8 cm	warm-season turfgrass	Bermudagrass	68.63	137.57	44.15	3.15	0.75	1.66
IT8F_b	8 cm	cool-season turfgrass	Tall Fescue	3.83	22.35	7.29	2.07	0.59	0.61
IT14B	14 cm	warm-season turfgrass	Bermudagrass	134.63	247.94	44.82	4.67	1.99	2.62
IT14F	14 cm	cool-season turfgrass	Tall Fescue	14.77	95.91	32.45	5.83	2.53	1.57

**Table A2**

Canopy height before cutting at a specific date (cm).

No.	Substrate thickness	Species	Modelled specie sas:	24/7	6/8	20/8	3/9	17/9	15/10
IT8B	8 cm	warm-season turfgrass	Bermudagrass	13.85	21.29	13.42	8.06	7.21	6.37
IT8F_b	8 cm	cool-season turfgrass	Tall Fescue	8.62	13.01	9.64	7.83	7.31	6.20
IT14B	14 cm	warm-season turfgrass	Bermudagrass	20.27	24.83	13.58	9.08	8.87	7.54
IT14F	14 cm	cool-season turfgrass	Tall Fescue	10.77	17.90	12.36	8.65	8.86	7.32

## Appendix 2

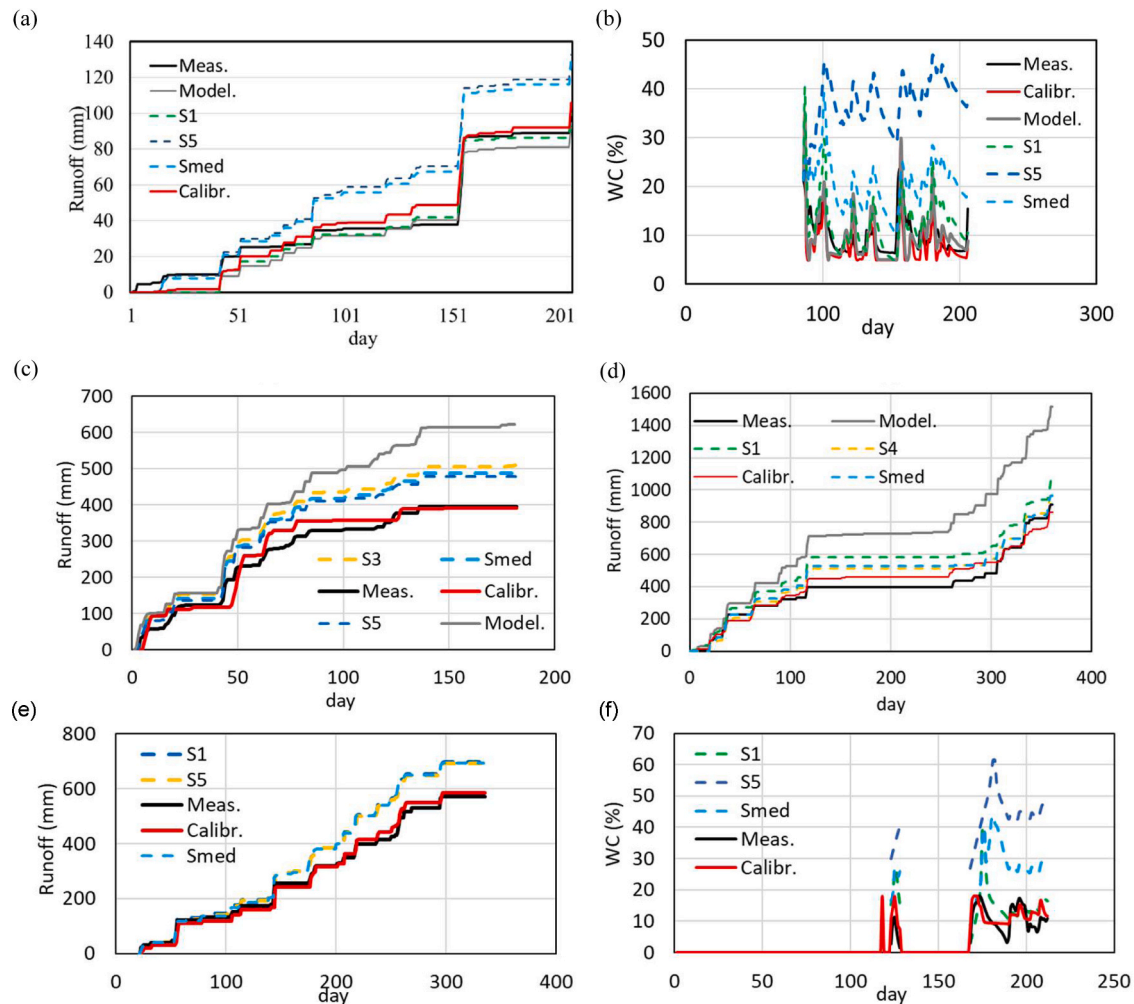


**Fig. A1.** Cumulative runoff or water content (WC) across the time series for data series CR5S (a and b), IT8F (c), IT15A (d), SL4S (e) and PT8S (f). “Model.” means modelled data, “Meas.” means measured data, “Calibr.” means calibrated values and the others refer to the representative European soils (“Smed” is the median of the results associated to the European soils).

## Appendix A. Supporting information

Supplementary data associated with this article can be found in the online version at [doi:10.1016/j.ufug.2024.128211](https://doi.org/10.1016/j.ufug.2024.128211).

## References

- Arkar, C., Domjan, S., Medved, S., 2018. Heat transfer in a lightweight extensive green roof under water-freezing conditions. *Energy Build.* 167, 187–199.
- Arnold, J.G., Moriasi, D.N., Gassman, P.W., Abbaspour, K.C., White, M.J., Srinivasan, R., Jha, M.K., 2012. SWAT: Model use, calibration, and validation. *Trans. of the ASABE* 55 (4), 1491–1508.
- Basu, A.S., Pilla, F., Sannigrahi, S., Gengembre, R., Guiland, A., Basu, B., 2021. Theoretical Framework to Assess Green Roof Performance in Mitigating Urban Flooding as a Potential Nature-Based Solution. *Sustainability* 13 (23), 13231.
- Broekhuizen, I., Sandoval, S., Gao, H., Mendez-Rios, F., Leonhardt, G., Bertrand-Krajewski, J., Viklander, M., 2021. Performance comparison of green roof hydrological models for full-scale field sites. *J. Hydrol.* X 12, 100093.
- Brudermann, T., Sangkakool, T., 2017. Green roofs in temperate climate cities in Europe – an analysis of key decision factors. *Urban For. Urban Green.* 21, 224–234.
- Catalano, C., Laudicina, V., Baudalucco, L., Guarino, R., 2018. Some European green roof norms and guidelines through the lens of biodiversity: do ecoregions and plant traits also matter? *Ecol. Eng.* 115, 15–26.
- Chaibou Begou, J., Jomaa, S., Benabdallah, S., Bazie, P., Afouda, A., Rode, M., 2016. Multi-site validation of the SWAT model on the Bani catchment: Model performance and predictive uncertainty. *Water* 8 (5), 178.
- Cristiano, E., Urru, S., Farris, S., Ruggiu, D., Deidda, R., Viola, F., 2020. Analysis of potential benefits on flood mitigation of a CAM green roof in Mediterranean urban areas. *Build. Environ.* 183, 107179.
- Culpepper, T., Young, J., Montague, D., Sulliva, D., Wherley, B., 2019. Physiological responses in C3 and C4 turfgrasses under soil water deficit. *HortScience* 54 (12), 2249–2256. 54(12, 2249–2256).
- Djedjig, R., Ouldboukhithine, S., Belarbi, R., Bozonnet, E., 2012. Development and validation of a coupled heat and mass transfer model for green roofs. *Int. Commun. Heat. Mass Transf.* 39 (6), 752–761.
- European Commission, 2010. Energy Performance of buildings (recast). *J. Eur. Union* 2010 (153), 13–35.
- European Commission. (2019a). The future of cities - Opportunities, challenges and the way forward. *EUR 29752 EN, JRC116711*.
- European Commission. (2019b). *Commission Staff Working Document, Guidance on a Strategic Framework for Further Supporting the Deployment of EU Level Green and Blue Infrastructure*. SWD/2019/193; European Union: Brussels, Belgium.
- European Commission. (2020). Communication from the Commission to the European Parliament, the Council, the European economic and social committee and the committee of the Regions EU Biodiversity Strategy for 2030 Bringing nature back into our lives. *COM/2020/380 final*.

- FLL, 2018. Green Roof Guidelines: Guidelines for the Planning, Construction and Maintenance of Green Roofs. Landscape Development and Landscaping Research Society e.V., Bonn.
- Giolo, M., Pornaro, C., Onofri, A., Macolino, S., 2020. Seeding time affects bermudagrass establishment in the transition zone environment. *Agron.* 10 (8), 1151.
- Gómez de Barreda, D., Azcárraga, C., Pornaro, C., 2022. Performance of turf-type bermudagrass cultivars in the upper and lower limits of the European transition zone, 114 (6), 3544–3553.
- Göşner, D., Mohri, M., Krespach, J.J., 2021. Evapotranspiration measurements and assessment of driving factors: a comparison of different green roof systems during summer in Germany. *Land* 10, 1334.
- Grădinaru, S., Hersperger, A., 2019. Green infrastructure in strategic spatial plans: evidence from European urban regions. *Urban For. Urban Green.* 40, 17–28.
- Griffith, S., Bamberger, M., 2001. Tall and fine fescue: relationship between growing degree days, developmental stage, and nitrogen acquisition. *Oregon State Univ., Corvallis.*
- Hansen, B., Schjønning, P., Sibbesen, E., 1999. Roughness indices for estimation of depression storage capacity of tilled soil surfaces. *Soil Tillage Res.* 52 (1–2), 103–111.
- He, H., Jim, C., 2010. Simulation of thermodynamic transmission in green roof ecosystem. *Ecol. Model.* 221 (24), 2949–2958.
- Jelinkova, V., Dohnal, M., Pícek, T., 2015. A green roof segment for monitoring the hydrological and thermal behaviour of anthropogenic soil systems. *Soil Water Res.* 10 (4), 262–270.
- Johannessen, B., Hanslin, H., Muthanna, T., 2017. Green roof performance potential in cold and wet regions. *Ecol. Eng.* 106, 436–447.
- Kozak, J.A., Ahuja, L.R., Green, T.R., Ma, L., 2007. Modelling crop canopy and residue rainfall interception effects on soil hydrological components for semi-arid agriculture. *Hydrol. Process.* 21 (2), 229–241.
- Kumar, R., Kaushik, S., 2005. Performance evaluation of green roof and shading for thermal protection of buildings. *Build. Environ.* 40 (11), 1505–1511.
- Lai, G., Luo, J., Li, Q., Pan, R., Zeng, X., Yi, F., 2020. Modification and validation of the SWAT model based on multi-plant growth mode, a case study of the Meijiang River Basin, China. *J. Hydrol.* 585, 124778.
- Liu, W., Engel, B., Feng, Q., 2021. Modelling the hydrological responses of green roofs under different substrate designs and rainfall characteristics using a simple water balance model. *J. Hydrol.* 602, 126786.
- Neitsch, S.L., Arnold, J.G., Kiniry, J.R., Williams, J.R., 2011. Soil and water assessment tool theoretical documentation version. Texas Water Resources Institute.
- Nektarios, P.A., Amountzias, I., Kokkinou, I., Ntoulas, N., 2011. Green roof substrate type and depth affect the growth of the native species *Dianthus fruticosus* under reduced irrigation regimens. *Hortic. Sci.* 46 (8), 1208–1216.
- Ntoulas, N., Nektarios, P.A., 2015. *Paspalum vaginatum* drought tolerance and recovery in adaptive extensive green roof systems. *Ecol. Eng.* 82, 189–200.
- Palermo, S., Turco, M., Principato, F., Piro, P., 2019. Hydrological effectiveness of an extensive green roof in Mediterranean climate. *Water* 11 (7), 1378.
- Palla, A., Gnecco, I., Lanza, L., 2009. Unsaturated 2D modelling of subsurface water flow in the coarse-grained porous matrix of a green roof. *J. Hydrol.* 379 (1–2), 193–204.
- Palla, A., Gnecco, I., Lanza, L., 2012. Compared performance of a conceptual and a mechanistic hydrologic models of a green roof. *Hydrol. Process.* 26 (1), 73–84.
- Paraskevopoulou, A., Mitsios, I., Fragkakos, I., Nektarios, P., Ntoulas, N., Londra, P., Papafotiou, M., 2015. The growth of *Arthrocnemum macrostachyum* and *Halimione portulacoides* in an extensive green roof system under two watering regimes. *Agric. and agric. sci. procedia* 4, 242–249.
- Patton, A.J., Hardebeck, G.A., Williams, D.W., Reicher, Z.J., 2004. Establishment of bermudagrass and zoysiagrass by seed. *Crop Sci.* 44 (6), 2160–2167.
- Pistocchi, A., Bauraoui, F., Bittelli, M., 2008. A simplified parameterization of the monthly topsoil water budget. *Water Resour. Res.* 44 (12).
- Quaranta, E., Dorati, C., Pistocchi, A., 2021. Meta-models for rapid appraisal of the benefits of urban greening in the European context. *J. Hydrol.: Reg. Stud.* 34, 100772.
- Quaranta, E., Dorati, C., Pistocchi, A., 2021. Water, energy and climate benefits of urban greening throughout Europe under different climatic scenarios. *Sci. Rep.* 11 (1), 1–10.
- Quaranta, E., Fuchs, S., Liefting, H.J., Schellart, A., Pistocchi, A., 2022. Costs and benefits of combined sewer overflow management strategies at the European scale. *J. Environ. Manag.* 318, 115629.
- Quaranta, E., Fuchs, S., Liefting, H.J., Schellart, A., Pistocchi, A., 2022. A hydrological model to estimate pollution from combined sewer overflows at the regional scale: application to Europe. *J. Hydrol.: Reg. Stud.* 41, 101080.
- Quezada-García, S., Espinosa-Paredes, G., Polo-Labarríos, M., Espinosa-Martínez, E., Escobedo-Izquierdo, A., 2020. Green roof heat and mass transfer mathematical models: a review. *Build. Environ.* 170, 106634.
- Rocha, B., Paco, T., Luz, A., Palha, P., Milliken, S., Kotzen, B., de Carvalho, R., 2021. Are biocrusts and xerophytic vegetation a viable green roof typology in a Mediterranean climate? A comparison between differently vegetated green roofs in water runoff and water quality. *Water* 13 (1), 94.
- Rosado-García, M., Kubus, R., Argüelles-Bustillo, R., García-García, M., 2021. A new european bauhaus for a culture of transversality and sustainability. *Sustainability* 13 (21), 11844.
- Sailor, D., Hutchinson, D., Bokovoy, L., 2008. Thermal property measurements for ecoroof soils common in the western U.S. *Energy Build.* 40 (7), 1246–1251.
- Shafique, M., Kim, R., Rafiq, M., 2018. Green roof benefits, opportunities and challenges—a review. *Renew. Sustain. Energy Rev.* 90, 757–773.
- Skala, V., Dohnal, M., Votruba, J., Vogel, T., Dusek, J., Sacha, J., Jelinkova, V., 2020. Hydrological and thermal regime of a thin green roof system evaluated by physically-based model. *Urban For. Urban Green.* 48, 126582.
- Soulis, K., Ntoulas, N., Nektarios, P., Kargas, G., 2017a. Runoff reduction from extensive green roofs having different substrate depth and plant cover. *Ecol. Eng.* 102, 80–89.
- Soulis, K., Valiantzas, J., Ntoulas, N., Kargas, G., Nektarios, P., 2017b. Simulation of green roof runoff under different substrate depths and vegetation covers by coupling a simple conceptual and a physically based hydrological model. *J. Environ. Manag.* 200, 434–445.
- Van Mechelen, C., Dutoit, T., Hermy, M., 2015. Adapting green roof irrigation practices for a sustainable future: A review. *Sustain. Cities Soc.* 19, 74–90.
- Van Renterghem, T., Botteldooren, D., 2014. Influence of rainfall on the noise shielding by a green roof. *Build. Environ.* 82, 1–8.
- Vanuytrecht, E., Van Mechelen, C., Van Meerbeek, K., Willems, P., Hermy, M., Raes, D., 2014. Runoff and vegetation stress of green roofs under different climate change scenarios. *Landsc. Urban Plan.* 122, 68–77.
- Varela-Stasinopoulou, D.S., Nektarios, P.A., Ntoulas, N., Trigás, P., Roukounakis, G.I., 2023a. Sustainable Growth of Medicinal and Aromatic Mediterranean Plants Growing as Communities in Shallow Substrate Urban Green Roof Systems. *Sustain.* 15 (7), 5940.
- Varela-Stasinopoulou, D.S., Nektarios, P.A., Tsanakas, G.F., Ntoulas, N., Roukounakis, G. I., Economou, A.S., 2023b. Impact of substrate depth and irrigation regime on growth, flowering and physiological indices of Greek sage (*Salvia fruticosa* Mill.) grown on urban extensive green roof systems. *Ecol. Eng.* 186, 106816.
- Versini, P., Gires, A., Tchiguirinskaia, I., Schertzer, D., 2020. Fractal analysis of green roof spatial implementation in European cities. *Urban For. Urban Green.* 49, 126629.
- Vijayaraghavan, K., 2016. Green roofs: A critical review on the role of components, benefits, limitations and trends. *Renew. Sustain. Energy Rev.* 57, 740–752.
- Wang, K., Dickinson, R., 2013. Global atmospheric downward longwave radiation at the surface from ground-based observations, satellite retrievals, and reanalyses. *Rev. Geophys.* 51, 150–185.
- Yan, J., Zhang, S., Zhang, J., Zhang, S., Zhang, C., Yang, H., Wei, L., 2022. Stormwater retention performance of green roofs with various configurations in different climatic zones. *J. Environ. Manag.*, 115447.
- Yang, W., Li, D., Sun, T., Ni, G., 2015. Saturation-excess and infiltration-excess runoff on green roofs. *Ecol. Eng.* 74, 327–336.
- Zapalowicz, Z., 2018. Simplified methodology to estimate the emissivity for roof covers. *E3S Web Conf.* 70 (6), 01021.